Optics Communications 334 (2015) 240–246

Contents lists available at ScienceDirect

Optics Communications

journal homepage: www.elsevier.com/locate/optcom

Compact device employed a hybrid plasmonic waveguide for polarization-selective splitting

Bing Sun [a], Yiping Wang [a,*], Yingjie Liu [a], Shen Liu [a], Changrui Liao [a], Ming-Yang Chen [b]

[a] Key Laboratory of Optoelectronic Devices and Systems of Ministry of Education and Guangdong Province, College of Optoelectronic Engineering, Shenzhen University, Shenzhen 518060, China

[b] Department of Optical Engineering, School of Mechanical Engineering, Jiangsu University, Zhenjiang 212013, Jiangsu Province, China

ARTICLE INFO

Article history:
Received 1 July 2014
Received in revised form
3 August 2014
Accepted 6 August 2014
Available online 20 August 2014

Keywords:
Coupler
Optical waveguide devices
Optical polarization
Plasmonic

ABSTRACT

We proposed an ultra compact polarization beam splitter (PBS) with a short coupling length of 2.82 μm consisting of a horizontally slotted waveguide (HSWG) and a hybrid plasmonic waveguide (HPWG). Only the TM-polarized mode can be supported in the HPWG, and the effective index, corresponding to the TM-polarized mode, in the HPWG is similar to that in the HSWG within a wide wavelength range. Consequently, the TM-polarized mode in the HSWG could be coupled into that in the HPWG. As a result, the TE- and TM-polarized modes are split. Such a PBS exhibits a high extinction ratio of up to −20 dB within an ultra wide wavelength range of 130 nm. Moreover, fabrication tolerances of the PBS are investigated.

1. Introduction

Silicon-on-insulator (SOI) technology has attracted lots of interests as a platform for guiding and manipulating optical signals in photonic integrated circuits. However, SOI waveguides involve highly polarization-dependent guiding owing to the high index difference between silicon and air/silica. As a result, the implementations of polarization beam splitters (PBSs) are essential in the applications of SOI waveguides. Although various configurations, such as multimode interference structures [1–3], Mach-Zehnder interferometers [4–6], photonic crystal structures [7,8], have been demonstrated to split polarization modes, one would prefer to implement PBSs based on directional couplers [9–22] due to their simplicity and easy design. For instance, Dai et al. [14] demonstrated an ultrashort polarization splitter with a strip-nanowire and a vertically slotted waveguide, which took advantage of the completely phase-matching condition for the TM polarization, while significantly suppressed the coupling for the TE polarization. Zhang, et al. presented a compact and efficient PBS using horizontally slotted waveguides with extinction ratio across C+L broadband [15]. Recently, a directional coupler, consisting of a vertically slotted waveguide and a channel waveguide, has been developed to realize polarization splitting with high extinction ratio of 20 dB for through port [16].

In recent years, plasmonic waveguides [23] have attracted intensive research interest due to their excellent ability to break the diffraction limit. Among them, hybrid plasmonic waveguides (HPWGs) are emerging because of their unique advantages of both long propagation length and strong confinement, and, in particular, large birefringence [24–28]. Recently, we demonstrated an on-chip PBS based on directional coupling system consisting of a horizontally slotted waveguide (HSWG) and a HPWG [18], in which only one polarization state was index-matched, whereas the index difference was very high for another polarization so that the effective coupling between the two polarization modes was prevented. Almost at the same time, Gao et al. [19] presented an ultracompact PBS consisting of a HPWG and a strip dielectric waveguide, which showed an extinction ratio of over 14.7 dB for the TE-polarized mode within the whole C band. In addition, Lou et al. [20] demonstrated a compact PBS based on a dielectric-hybrid plasmonic-dielectric coupler. In the meanwhile, Chee et al. [21] designed a similar device by use of Cu as the metal cap and demonstrated an ultrashort integrated polarization splitter with a bandwidth of more than 70 nm and an extinction ratio of less than 15 dB. An asymmetrical coupling system consisting of a hybrid plasmonic waveguide and a silicon nanowire has been proposed by Guan et al. [22].

In this paper, we present a promising PBS based on a directional coupling system consisting of a HSWG and a HPWG. Such a PBS is optimally designed to satisfy the phase-matching condition for TM-polarized modes of the two waveguides, while the TE-polarized mode cannot be supported in the HPWG. In the

* Corresponding author.
E-mail address: ypwang@szu.edu.cn (Y. Wang).

http://dx.doi.org/10.1016/j.optcom.2014.08.014
0030-4018/

proposed PBS, the two index-curves of the TM-polarized modes in the HSWG and the HPWG have a very small index difference so that strong coupling occurs within a wide wavelength range. In contrast, the effective coupling for the TE-polarized mode is prevented due to the fact that only TM-polarized guided mode can be supported in the HPWG. Consequently, our PBS could be used to split the TM- and TE-polarized modes with a high extinction ratio within an ultra wide wavelength range.

2. Numerical simulation

As shown in Fig. 1, we designed a PBS consisting of a HSWG with a width of w and a HPWG with a width of w_h. The HSWG is composed of a silica spacer with a thickness of h_{slot} and two silicon layers with a thickness of h_s. The HPWG is composed of a metal layer, a silica spacer, and a silicon layer with a thickness of h_m, h_d, and h, respectively. The gap distance between the two waveguides is defined as d. The substrate of the PBS is assumed to be silica with a refractive index of 1.4500. Refractive index of silicon ($n_{silicon}$) is 3.4764. Gold is chose to be the metal layer of the HPWG and its permittivity can be given by [29].

$$\varepsilon_{Au}(\lambda)=\varepsilon_{\infty}-\frac{1}{\lambda_p^2(1-\lambda^2+i/\lambda_p\lambda)}+\sum_{j=1,2}\frac{A_j}{\lambda_j}\left[\frac{e^{i\phi_j}}{(1/\lambda_j-1/\lambda+i/\lambda_j)}+\frac{e^{-i\phi_j}}{(1/\lambda_j+1/\lambda-i/\lambda_j)}\right] \tag{1}$$

where the first and second terms are the contribution from the Drude model, and the third and fourth terms are the contribution from the interband transitions. The parameters in Eq. (1) are listed in Table 1. The default operation wavelength is 1550 nm.

Fig. 2 illustrates the calculated effective refractive indices (N_{eff}) and propagation distances of the TM-polarized mode in the HPWG as a function of the HPWG width of w_h, where the propagation distance of the TM- and TE-polarized modes is defined as a distance over which the guided power drops to 1/e of its initial magnitude. As shown in Fig. 2(a) and (b), the effective index and the propagation length of the TE-polarized mode decreases and increases, respectively, with the decrease of w_h. It can be seen from that the TE-polarized mode is gradually coupled into the silica substrate with the decreases of w_h (Fig. 2(e)), while the TE-polarized mode is confined in the HPWG (Fig. 2(f)). Simulation results show that the TE-polarized mode is completely leaked into the silica substrate while w_h is less than 240 nm. In other words, the TE-polarized mode cut off in the HPWG with a width of less than 240 nm. On the other hand, as shown in Fig. 2(c) and (d), both the effective index and the propagation length of the TM-polarized mode decrease with the decrease of w_h. We also calculated the effective refractive indices and the propagation lengths of the TM- and TE-polarized modes in the HPWG with different silica spacer thicknesses, h_d, of 60, 80, and 100 nm in order to find an optimal silica spacer thickness of 80 nm, as described below.

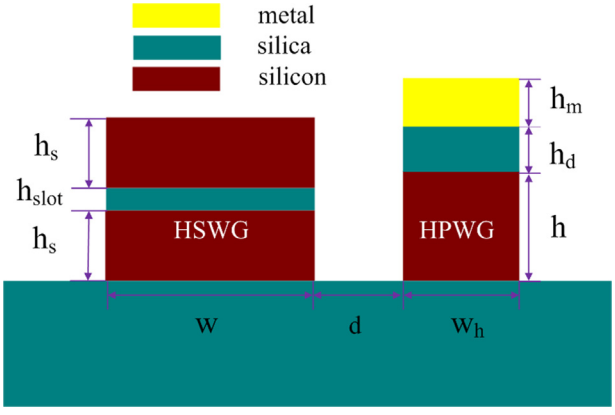

Fig. 1. Schematic diagram of the cross section of a proposed PBS consisting of a HSWG and a HPWG.

As shown in Fig. 3(a), the refractive index differences between the TM- and TE-polarized modes in the HSWG with a silicon layer thickness of 150 nm and a silica layer thickness (h_s) of 30, 45, and 50 nm are 0.568608, 0.592991 and 0.596920, respectively, at the wavelength of 1550 nm. As shown in Fig. 3(b), in case the silicon layer thickness is 200 nm, the refractive index differences above are decreased by 0.384813, 0.444664 and 0.459149, respectively. As a result, smaller silicon layer thickness and larger silica layer thickness are best except larger silica layer thickness may lead to higher order guided-modes.

Based on the above analysis, we improve the parameters of the desired PBS to be w=450 nm, w_h=200 nm, h_m=100 nm, h_d=80 nm, h_{slot}=36.5 nm, h=250 nm, h_s=150 nm, and d=100 nm. The parameters above will be used in all simulations below. We calculated the effective indices of the fundamental modes in a HSWG and a HPWG with the parameters above, as shown in Fig. 4. Obviously, only the TM-polarized mode can be supported in the HPWG. It can be easily found from Fig. 4 that the index difference between the TM-polarized modes of the two waveguides is very small in an ultra wide wavelength range from 1.45 μm to 1.65 μm. Therefore, the TM-polarized modes in the HSWG and the HPWG are index-matched in the wide wavelength range. On the other hand, the evanescent coupling of the TE-polarized light is entirely suppressed due to the cutoff of the TE-polarized mode in the HPWG.

The reason for choosing a HSWG, rather than a single silicon waveguide (SWG) could be described as follow. As shown in Fig. 5, although the HSWG and the SWG have the same index-matching point with the HPWG, each waveguide exhibits different index curves. And effective index difference of the TM-polarized modes between the SWG and the HPWG is quite larger than that between the HSWG and the HPWG. As a result, the coupling efficiency of the TM-polarized mode from the HSWG to the HPWG is much higher than that from the SWG to the HPWG [30]. So a HSWG, rather than a SWG, is integrated in our PBS.

Operation principle of our PBS could also be explained in terms of the supermode theory for the TM-polarized modes. In case each core of a coupler is a single-mode-guided waveguide, such a coupler structure can support two modes, including one odd mode and one even mode, and the coupling length, L, can be calculated by:

$$L_c^{TM}=\frac{\lambda}{2(n_e{}^{TM}-n_o{}^{TM})} \tag{2}$$

where $n_e{}^{TM}$ and $n_o{}^{TM}$ are the effective indices of the even and odd supermodes, respectively. Electric field distributions of the guided modes in the PBS with a gap distance of 100 nm were simulated by finite element method. As shown in Figs. 6(a) and (b), antisymmetric

Table 1
Parameters used in Eq. (1) for gold.

Parameter (units)	Data of Johnson and Christy
ε_{∞}	1.54
λ_p(nm)	143
γ_p(nm)	14500
A_1	1.27
ϕ_1(rad)	$-\pi/4$
λ_1(nm)	470
γ_1(nm)	1900
A_2	1.4
ϕ_2 (rad)	$-\pi/4$
λ_2(nm)	325
γ_2(nm)	1060

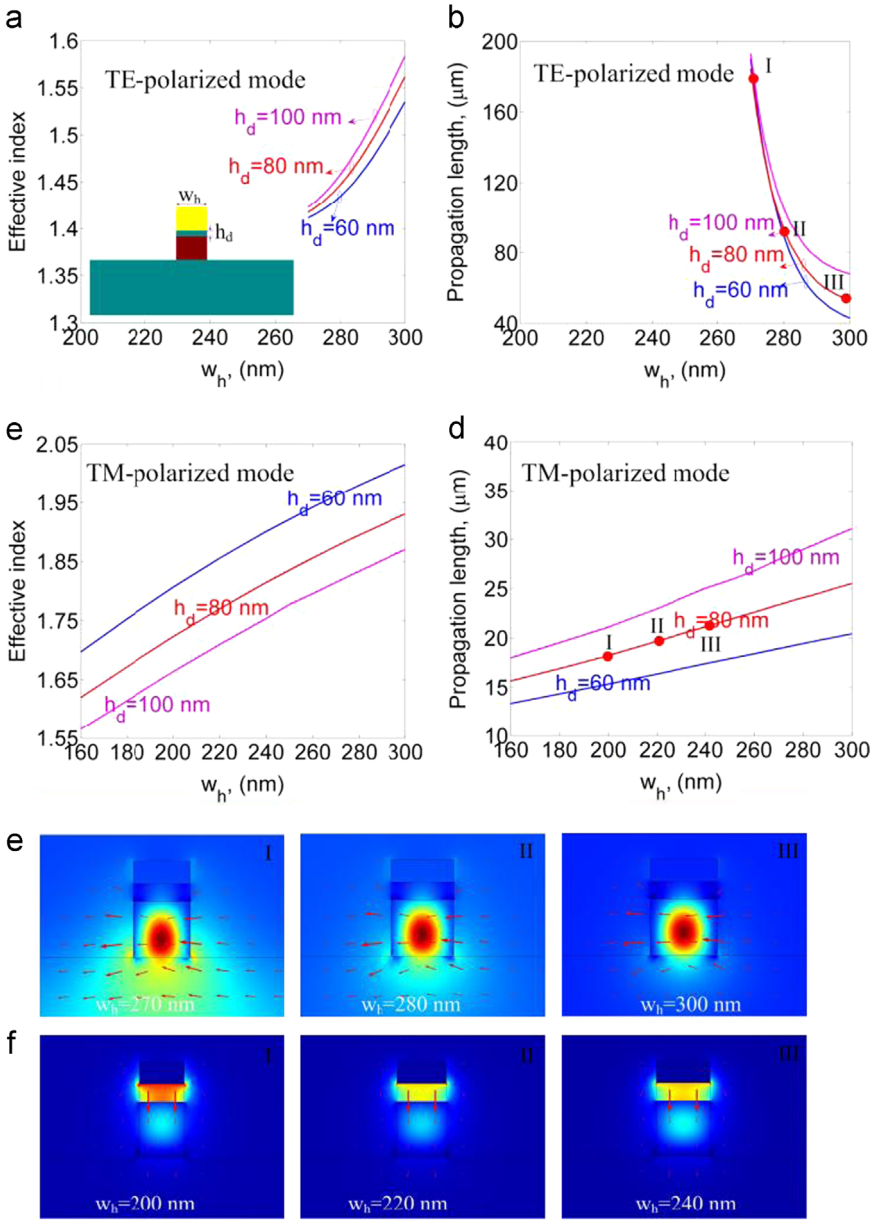

Fig. 2. (a) and (b) effective refractive index (N_{eff}), and (c) and (d) propagation distance of the TM- and TE-polarized modes, respectively, as a function of the width, w_h, in the HPWG with different silica spacer thicknesses, h_d, of 60, 80 , and 100 nm. Other parameters are h_m=100 nm, h=250 nm. Operation wavelength is 1550 nm. Fig.2(e) and (f) illustrate mode filed profiles corresponding to different width, w_h in the case of h_d=80 nm.

and symmetric TM-polarized supermodes can be simultaneously supported in the PBS. As shown in Fig. 6(c), whereas, only the TE-polarized supermode can be supported in the HPWG.

Fig. 7 illustrates the energy of the TM- and TE-polarized modes at the output end of the HSWG when light is launched at the input end of the HSWG. It can be found from the blue curve illustrated in Fig. 7 that the normalized optical intensity of the TM-polarized mode is periodically modulated in the HSWG. In case light transmits to a length of 2.82 μm, the optical intensity is decreased to zero. That is, the TM- and TE-polarized modes can be completely separated. Such a length is the so-called coupling length of the TM-polarized modes. Although the metal employed will result in a transmission loss, the loss is very small in the PBS because such a device has a very short length of 2.82 μm. Our simulation shows the metal-induced losses of the TE- and TM-polarized modes, are only 0.08 and 0.17 dB, respectively.

Extinction ratios of the TM- and TE-polarized modes, i.e. ER_{TM} and ER_{TE}, are defined as the energy ratio between the undesired and the desired polarized mode at the output end of the HPWG and the HSWG, respectively. As shown in Fig. 8, ER_{TM} and ER_{TE} at the output end of the HPWG and the HSWG are up to −41 dB and −33 dB at the wavelength of 1550 nm, respectively. Moreover, ER_{TM} at the output end of the HPWG is more than −20 dB within the wavelength range from 1490 to 1620 nm, ER_{TE} at the output end of the HSWG is more than -25 dB at each wavelength. Therefore, the extinction ratios of both the TM- and TE-polarized modes are more than −20 dB over an ultra-wide wavelength range of 130 nm.

The HPWG and the HSWG have different transmission loss. For example, the complex refractive indices of the even and odd supermodes are calculated as 1.601073+0.004801i and 1.875172+0.00256i at λ=1.55 μm, respectively. As a result, the propagation lengths are calculated via $L_m=1/[2\mathrm{Im}(\beta)]$ as 25.6 μm and 48.1 μm, respectively. Accordingly, the TM-polarized mode remained in the HPWG only undergo a litter transmission loss owing to the small size (2.82 μm). Moreover, the transmission

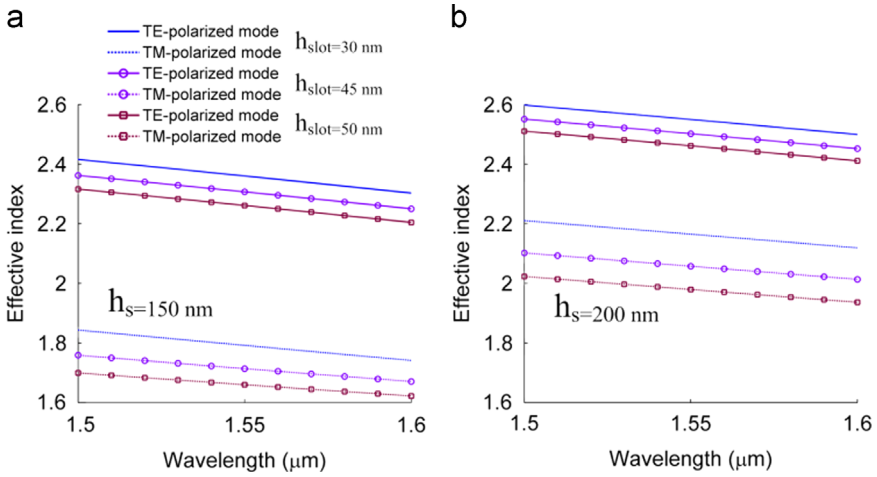

Fig. 3. Effective index (N_{eff}), corresponding to the TM- and TE-polarized modes, as a function of wavelength in the HSWG with a silicon layer thickness (h_s) of (a) 150 nm and (b) 200 nm and different silica layer thickness (h_{slot}) of 30, 45, 50 nm.

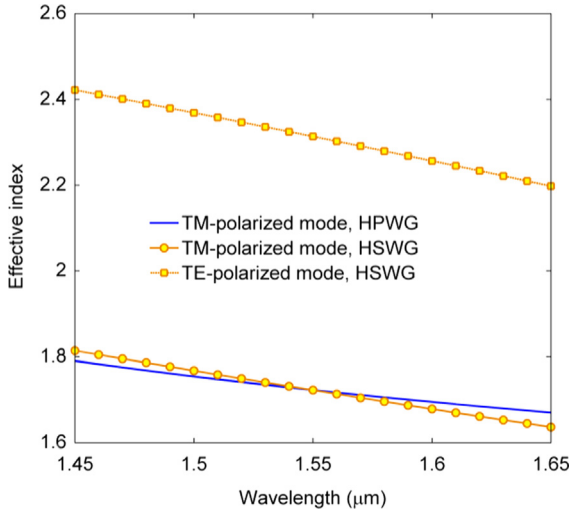

Fig. 4. Effective indices versus wavelength in the HSWG and the HPWG with improved parameters.

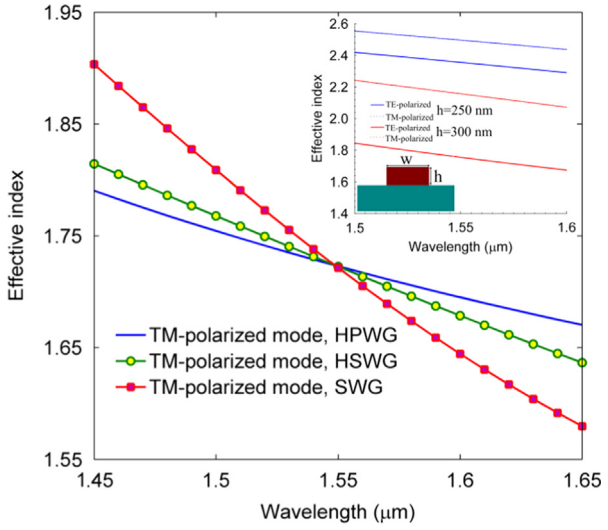

Fig. 5. Effective refractive indices, N_{eff}, versus wavelength in a SWG, a HSWG, and a HPWG. Inset shows N_{eff} of a SWG with a width of 450 nm versus wavelength.

losses of the TE-polarized mode is nearly zero, and that of the TM-polarized mode is less than 0.5 dB within a wide wavelength from 1450 nm to 1650 nm, as shown in Fig. 8.

As well-known, the properties of an optical waveguide strongly depend on the device dimension and size. We calculated the extinction ratios of the TM- and TE-polarized modes at the wavelength of 1550 nm while the silica layer thickness of the HPWG (h_d), the silicon layer thickness of the HSWG (h_s), the width of the HSWG (w) are changed by Δh_d, Δh_s, and Δw, respectively. As shown in Fig. 9, a good extinction ratio (more than -20 dB) of the TM-polarized mode can be achieved while the PBS has a size change of $-25\ \text{nm} < \Delta h_d < 35\ \text{nm}$, $-22\ \text{nm} < \Delta h_S < 30\ \text{nm}$, or $-21\ \text{nm} < \Delta w < 16\ \text{nm}$. Therefore, our PBS has an excellent size tolerance.

We will couple light to/from our proposed PBS by means of the same method reported in Ref. [21]. The light can be coupled to/from a hybrid plasmonic waveguide to a standard single-mode fiber through grating couplers with an insert loss of 2.8 dB and 6.0 dB for TE and TM modes, respectively, as described in Ref. [21] in which the waveguide employed is similar to our PBS. The grating couplers are used not only for high-efficiency fiber-chip coupling but also for the high extinction-ratio polarizer. Also it can be minimized through the improved coupling efficiency. Further investigation on the package for our PBS will done in the future.

In our previous publication [18], we presented a compact polarization beam splitter consisting of a horizontally slotted waveguide and a hybrid plasmonic waveguide. Such a splitter has a large difference between the effective indices of the TE-polarized modes in the two waveguides, while the effective index difference of the TM-polarized modes is quite small in a wide wavelength range. However, a coupling of the TE-polarized modes always happens between the two waveguides due to a litter weak phase matching so that the polarization splitter has a narrow bandwidth. Compared with the device reported in Ref. [18], we currently present an improved PBS configuration in which only the TM-polarized mode can be supported in the hybrid plasmonic waveguide. So the coupling of the TE-polarized modes cannot exist in the proposed PS. Furthermore, the effective index curves of the TM-polarized modes in the HSWG and the HPWG are improved to be very closely each other to achieve a phase-matching condition in a wide wavelength range. Consequently, the PBS has an

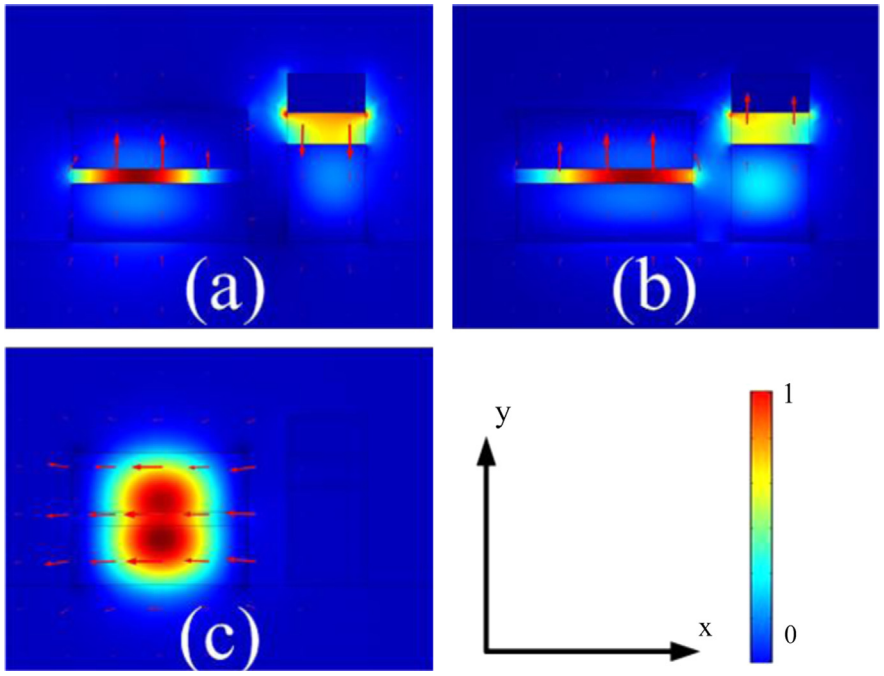

Fig. 6. Electric field profiles of (a) antisymmetric and (b) symmetric TM-polarized supermodes and (c) TE-polarized supermode at 1550 nm in the PBS.

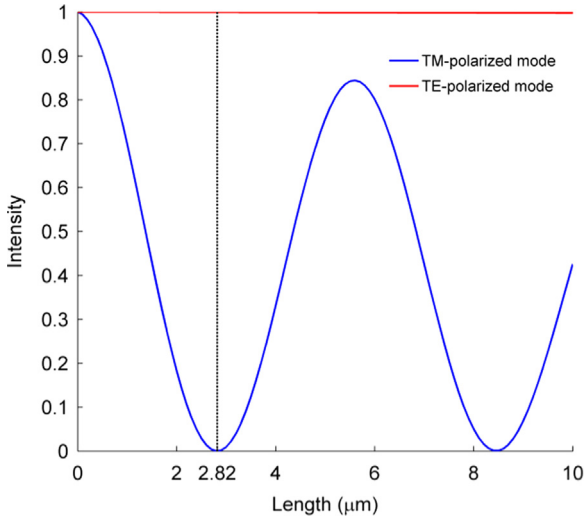

Fig. 7. The normalized optical intensities of the TM- and TE-polarized modes at the output end of the HSWG in case light is launched at the input end of the HSWG.

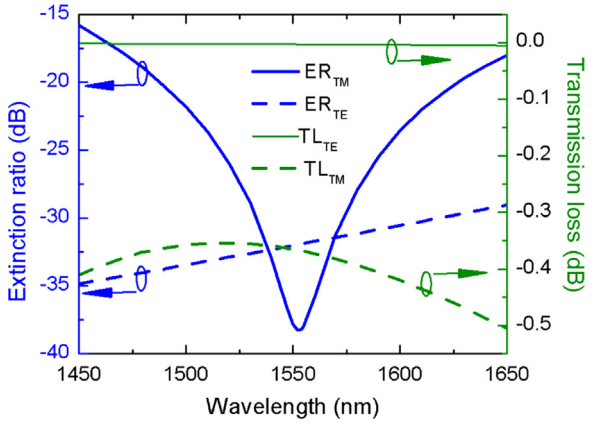

Fig. 8. Extinction ratios and transmission loss of the TM- and TE-polarized modes versus wavelength at the output end of the HPWG and the HSWG, respectively.

extinction ratio of more than −20 dB within an ultrawide bandwidth of 130 nm. Moreover, the proposed PBS is an ultracompact device with a short coupling length of 2.82 μm.

3. Discussion

3.1. The effect of bending waveguides

We have designed an output waveguide (a sharply bent HSWG) at the end of the coupling region to stop coupling light back. The bending radius (R) depends on the waveguide design and its bending loss. The length of the coupling region usually needed to be reduced to compensate the extra coupling in the beginning section of the bending region. The performance of our PBS was investigated by means of three dimensional finite-difference-time-domain (3D–FDTD) simulation [31]. The computational region is uniformly meshed in each direction and surrounded by the Perfectly Matched Layer boundary conditions. Figs. 10(a) and (b) show the simulated light propagation in the designed PBS with $R=1.3$ μm and $L_c=2.6$ μm for TE-polarized and TM-polarized modes at the wavelength of 1550 nm, respectively. The grid sizes are chosen as $\Delta x=15$ nm, $\Delta y=8$ nm, and $\Delta z=20$ nm. It can be seen from Fig. 10 that the TM-polarized light couples efficiently from the HSWG to the HPWG, while the TE-polarized light fully transmits in the HSWG.

3.2. Device fabrication

The designed splitter was fabricated together with other photonic and plasmonic devices on SOI wafers with top-Si and buried oxide. The reference [21] schematically described some key steps of fabrication flow. Providing these layer thicknesses are the

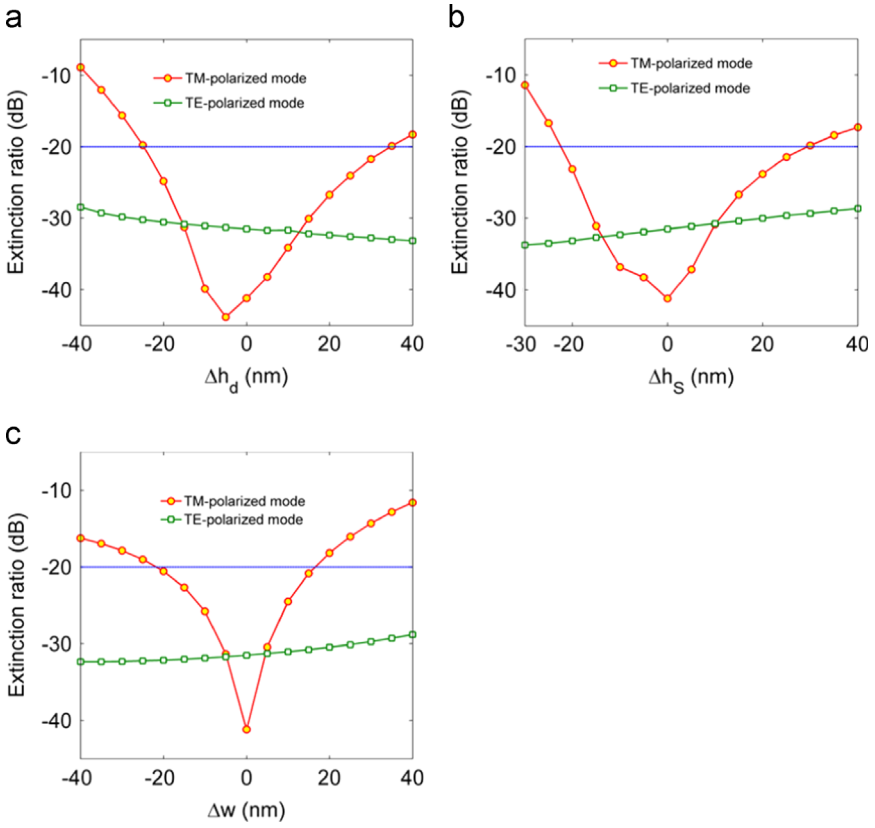

Fig. 9. Size tolerance of the designed device with variations (a) Δh_d, (b) Δh_s, and (c) Δw.

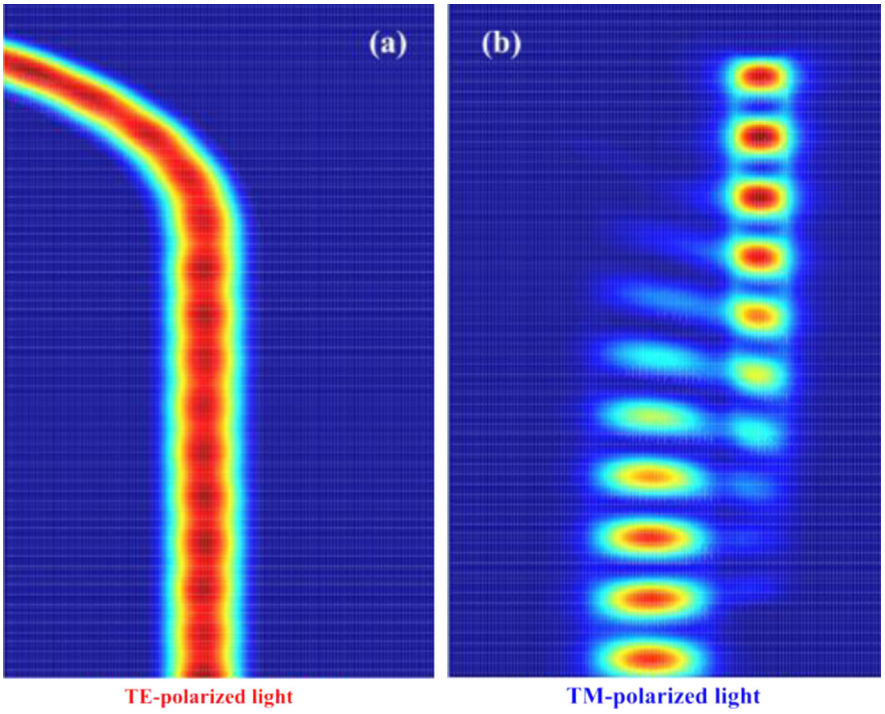

Fig. 10. FDTD propagation field profiles of the (a) TE- and (b) TM-polarized modes.

same, the device can be fabricated with less difficulty. But only the widths of the HSWG and the HPWG could be changed/improved so that such a device is with less flexibility and cannot realize the desired functions. Hence, our device has two different lower silicon (h, h_s) and silica layers (h_{slot}, h_d). However, we can further optimize the structure and make it be compatible.

4. Conclusion

We designed an ultracompact silicon-based PBS consisting of a horizontally slotted waveguide and a hybrid plasmonic waveguide. By the optimized procedure, the TM-polarized states of the HSWG and HPWG are index-matched in a wide wavelength range. On the

other hand, the evanescent coupling is significantly suppressed due to the fact that the TE-polarized state cannot be supported in the HPWG. In particular, our improved PBS has a very short coupling length of 2.82 μm and the extinction ratios of both the TM- and TE-polarized modes are more than −20 dB over a wide wavelength range of 130 nm.

Acknowledgments

This work was supported by the National Science Foundation of China (Grant no. 11174064, Grant no. 61377090, and Grant no. 61308027), the Science & Technology Innovation Commission of Shenzhen (Grant no. KQCX 20120815161 444632, and Grant no. JCYJ20130329140017262), and the Distinguished Professors Funding from Shenzhen University and Guangdong Province Pearl River Scholars.

References

[1] J.M. Hong, H.H. Ryu, S.R. Park, J.W. Jeong, S.G. Lee, E.-H. Lee, et al., Photon. Technol. Lett. IEEE 15 (2003) 72.
[2] A. Katigbak, J.F. Strother, J. Lin, Opt. Eng. 48 (2009) 080503.
[3] B.-K. Yang, S.-Y. Shin, D. Zhang, Photon. Technol. Lett. IEEE 21 (2009) 432.
[4] T. Liang, H. Tsang, Photon. Technol. Lett. IEEE 17 (2005) 393.
[5] L. Augustin, R. Hanfoug, J. van der Tol, W. de Laat, M. Smit, Photon. Technol. Lett. IEEE 19 (2007) 1286.
[6] D. Dai, Z. Wang, J. Peters, J. Bowers, Photon. Technol. Lett. IEEE (2011) 1.
[7] Y. Shi, D. Dai, S. He, Photon. Technol. Lett. IEEE 19 (2007) 825.
[8] X. Ao, L. Liu, L. Wosinski, S. He, Appl. Phys. Lett. 89 (2006) 171115.
[9] I. Kiyat, A. Aydinli, N. Dagli, Photon. Technol. Lett. IEEE 17 (2005) 100.
[10] X. Tu, S.S.N. Ang, A.B. Chew, J. Teng, T. Mei, Photon. Technol. Lett. IEEE 22 (2010) 1324.
[11] Y. Yue, L. Zhang, J.Y. Yang, R.G. Beausoleil, A.E. Willner, Opt. Lett. 35 (2010) 1364.
[12] K. Saitoh, M. Koshiba, Opt. Express 17 (2009) 19225.
[13] S. Lin, J. Hu, K.B. Crozier, Appl. Phys. Lett. 98 (2011) 151101.
[14] D. Dai, Z. Wang, J.E. Bowers, Opt. Lett. 36 (2011) 2590.
[15] H. Zhang, Y. Huang, S. Das, C. Li, M. Yu, P.G.-Q. Lo, et al., Opt. Express 21 (2013) 3363.
[16] J. Wang, J. Xiao, X. Sun, J. Opt. 15 (2013) 035501.
[17] Q. Li, Y. Song, G. Zhou, Y. Su, M. Qiu, Opt. Lett. 35 (2010) 3153.
[18] B. Sun, M.-Y. Chen, Y.-K. Zhang, J. Zhou, Appl. Phys. B 113 (2013) 179.
[19] L. Gao, F. Hu, X. Wang, L. Tang, Z. Zhou, Appl. Phys. B 113 (2013) 199.
[20] F. Lou, D. Dai, L. Wosinski, Opt. Lett. 37 (2012) 3372.
[21] J. Chee, S. Zhu, G. Lo, Opt. Express 20 (2012) 25345.
[22] X. Guan, H. Wu, Y. Shi, L. Wosinski, D. Dai, Opt. Lett. 38 (2013) 3005.
[23] D.K. Gramotnev, S.I. Bozhevolnyi, Nat. Photon. 4 (2010) 83.
[24] R.F. Oulton, V.J. Sorger, D. Genov, D. Pile, X. Zhang, Nat. Photon. 2 (2008) 496.
[25] D. Dai, S. He, Opt. Express 17 (2009) 16646.
[26] M. Wu, Z. Han, V. Van, Opt. Express 18 (2010) 11728.
[27] L. Gao, L. Tang, F. Hu, R. Guo, X. Wang, Z. Zhou, Opt. Express 20 (2012) 11487.
[28] M.Z. Alam, J.S. Aitchison, M. Mojahedi, IEEE J. Sel. Top.Quantum Electron. 19 (2013) 4602008.
[29] P.G. Etchegoin, E.C.L. Ru, M. Meyer, J. Chem. Phys. 125 (2006) 164705.
[30] B. Sun, M.-Y. Chen, Y.-K. Zhang, J.-C. Yang, J.-Q. Yao, H.-X. Cui, Opt. Express 19 (2011) 4091.
[31] G. Seniutinas, L. Rosa, G. Gervinskas, E. Brasselet, S. Juodkazis, Beilstein J. Nanotechnol. 4 (2013) 534.